JOURNAL OF VIROLOGY, July 1993, p. 4337–4349
0022-538X/93/074337-13$02.00/0

Vol. 67, No. 7

Alterations of the Three Short Open Reading Frames in the Rous Sarcoma Virus Leader RNA Modulate Viral Replication and Gene Expression

ARISTIDIS MOUSTAKAS,[1]† TAD S. SONSTEGARD,[1] AND PERRY B. HACKETT[1,2]*

Department of Genetics and Cell Biology, University of Minnesota, St. Paul, Minnesota 55108-1095,[1] and Institute of Human Genetics, University of Minnesota, Minneapolis, Minnesota 55455[2]

Received 28 December 1992/Accepted 16 April 1993

The Rous sarcoma virus (RSV) leader RNA has three short open reading frames (ORF1 to ORF3) which are conserved in all avian sarcoma-leukosis retroviruses. Effects on virus propagation were determined following three types of alterations in the ORFs: (i) replacement of AUG initiation codons in order to prohibit ORF translation, (ii) alterations of the codon context around the AUG initiation codon to enhance translation of the normally silent ORF3, and (iii) elongation of the ORF coding sequences. Mutagenesis of the AUG codons for ORF1 and ORF2 (AUG1 and AUG2) singly or together delayed the onset of viral replication and cell transformation. In contrast, mutagenesis of AUG3 almost completely suppressed these viral activities. Mutagenesis of ORF3 to enhance its translation inhibited viral propagation. When the mutant ORF3 included an additional frameshift mutation which extended the ORF beyond the initiation site for the *gag*, *gag-pol*, and *env* proteins, host cells were initially transformed but died soon thereafter. Elongation of ORF1 from 7 to 62 codons led to the accumulation of transformation-defective virus with a delayed onset of replication. In contrast, viruses with elongation of ORF1 from 7 to 30 codons, ORF2 from 16 to 48 codons, or ORF3 from 9 to 64 codons, without any alterations in the AUG context, exhibited wild-type phenotypes. These results are consistent with a model that translation of the ORFs is necessary to facilitate virus production.

Three short open reading frames (ORF1 to ORF3) are contained in the 5′ leader RNA sequences of all known avian leukosis-sarcoma retroviruses (9, 24, 25, 33, 53). The lengths and the relative positions of the ORFs in the leader RNA sequence are highly conserved, but the encoded amino acid sequences are not (23, 24, 28). The nucleotides surrounding the initiation codons of each of the three ORFs are also conserved such that the first AUG codon is a favorable initiator of translation whereas the second and third AUG codons should be weaker sites of initiation (37, 50).

In previous studies of the wild-type (WT) Rous sarcoma virus (RSV) strain SR-A(SF), we demonstrated that the AUG codon of ORF1 is the major ribosome-binding site within the RSV 5′ leader (48–50). Furthermore, the seven-amino-acid product of ORF1 was identified in vitro (24), indicating productive protein synthesis from the ORF. Additional translational studies in vitro (29, 52) and in vivo (40, 42) have demonstrated that (i) either deletions of one or more ORFs or mutagenesis of their initiation codons had relatively minor effects on downstream gene translation, (ii) elongation of the ORFs resulted in reductions in downstream translation proportional to the extent of elongation, and (iii) mutation of the first AUG codon to ACG produced a virus with a delayed onset of propagation and cellular transformation (50). These studies suggested that (i) the 5′ leader RNA sequences of the multicistronic RSV mRNAs were scanned by ribosomal subunits (29, 48), (ii) ORF1 and ORF2, but not ORF3, were translated (24, 49, 50), and (iii) the mechanisms of leaky scanning (37) and reinitiation (32, 47) explained best the efficient initiation of translation at the AUG codons of the major viral genes (40). These effects on translation, plus the observation that ORF1 was required for efficient RSV replication (50), suggested that conservation of the ORF structures might be essential for maintaining essential activities during the life cycle of the virus. Another report (17), which emerged while our work was in progress, supports this hypothesis.

Accordingly, we studied in detail the effects that destruction and/or length alterations of the ORFs had on viral replication as well as on cellular viability and transformation. We found that inactivation of the AUG codons for ORF1 and ORF2 attenuated viral replication whereas certain alterations in ORF3 destroyed viral replication and/or simultaneously killed the host cell. Furthermore, extension of ORF1 to more than 60 codons delayed the onset of viral growth in a way similar to that seen when ORF1 was lost (50). However, shorter elongations of ORF1 to ORF3 had little effect on the virus. These results are consistent with our hypothesis that the ORFs in avian retrovirus leader RNA sequences are translated during infection and suggest that the ORFs are important for efficient viral propagation.

MATERIALS AND METHODS

Construction of recombinant RSV genomes carrying mutant ORFs. The in vitro, site-specific mutagenesis protocol, the mutagenesis procedure, and construction of recombinant RSV genomes have been described in detail elsewhere (42, 50). All mutations were screened by restriction endonuclease digests (GIBCO-BRL and New England Biolabs) and were verified by DNA sequencing after reconstruction of the final clones. Figure 1 depicts the ORF sequences that were mutagenized and the nomenclature of the recombinant clones.

Cell culture; transfection and reinfection of CEFs. Primary chicken embryo fibroblast (CEF) cultures were prepared

* Corresponding author.
† Present address: Whitehead Institute for Biomedical Research, Cambridge, MA 02142.

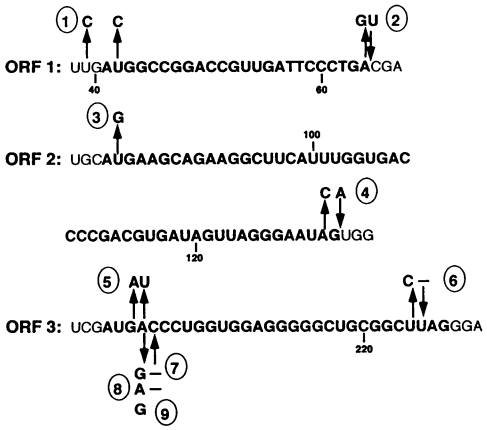

FIG. 1. Site-specific mutations of the RSV leader ORFs. The nucleotide sequences of the ORFs are shown in bold, with the flanking three bases at each end shown in lighter type. Mutations in the AUG codons or the flanking bases are shown by arrows. The mutations were nucleotide substitutions except for nucleotide deletions indicated by dashes (6, 7, and 8) and insertions indicated by arrows pointing downward between adjacent bases (2 and 4). Mutations were screened by alterations in restriction endonuclease cleavage sites. Mutation designations: 1, AUG1; 2, TC1; 3, AUG2; 4, TC2; 5, AUG3; 6, TC3; 7, FS3; 8, FS3R; 9, AUG3$^+$.

from 12-day, virus-free chicken embryos (SPF-COFAL/MAREK; SPAFAS, Inc.) and were maintained in M199 medium (GIBCO) supplemented with 10% tryptose phosphate broth (Sigma), 1% chicken serum (GIBCO), and 5% fetal bovine serum (HyClone Laboratories, Inc.). CEFs between passages 2 and 5 were transfected with 10 μg of linearized viral DNA per 100-mm-diameter tissue culture dish by using DEAE-dextran (Pharmacia) and either chloroquine (Sigma) or serum-free shock (40, 50, 57). Every independent transfection experiment included a positive control using the WT clone, a negative control of the vector DNA, pUC19, and a mock transfection lacking input of any DNA. Media collected from transfected plates were measured for reverse transcriptase activity so that equal virus titers could be used to reinfect fresh CEFs.

Soft agar assays. Fresh CEFs were plated in 60-mm-diameter gridded plates, infected with serially diluted viral stocks which were collected from the transfected cultures, and overlaid with agar (Difco) after overnight incubation for the focus assay (31). Foci (focus-forming units [FFU]) were scored 5 to 7 days postinoculation. Two plates per viral stock dilution were included in every independent experiment, and three experiments were run for each virus.

Reverse transcriptase assays. Culture medium from transfected or reinfected cells was clarified from cells by centrifugation at 2,000 × *g* for 10 min, and supernatant aliquots were assayed for reverse transcriptase under conditions described previously (22, 46). Incorporation of [^{32}P]dTMP (Amersham) into DNA was assayed by the DEAE filter-binding technique (22) followed by Cerenkov counting.

Isolation and analysis of RNAs. Total RNA was isolated from confluent infected cells (12), and formaldehyde-gel electrophoresis and RNA blotting analysis were performed (12, 50). The probes used for hybridization of the RNA blots were a full-size proviral 9.6-kbp DNA, a 450-bp *Hin*dIII-*Xba*I DNA fragment encoding the C terminus of the *env* polyprotein, and a 2-kbp chicken β-actin cDNA (13), which served as a control of the mRNA levels loaded on the gels. All probes were uniformly radiolabeled with [α-^{32}P]dATP (Amersham) by using random primers.

Analysis of Pr76^{gag} and pp60$^{v\text{-}src}$ production. CEFs were transfected as described above. Transfected CEFs were cultured 9 to 12 days prior to harvest. Immunoprecipitations were done as previously described by Wills et al. (57). Monolayers were labeled by incubation in 800 μl of methionine-free, serum-free medium (Sigma) containing 50 μCi of [^{35}S]methionine (specific activity, >1,100 Ci/mmol; ICN Biomedicals) for 2.5 h. Cell cultures were then fractionated in 1 ml of lysis buffer (25 mM Tris hydrochloride [pH 8.0], 0.15 M NaCl, 1% Triton X-100, 1% deoxycholate, 100 μg of phenylmethylsulfonyl fluoride per ml, 5 μg of pepstatin A per ml, 5 μg of leupeptin per ml) and incubated at 4°C for 8 h with either an anti-RSV antiserum (generously provided by J. Wills, Pennsylvania State University) or a monoclonal antibody for v-*src* (Oncogene Science). Protein-antibody complexes were collected with protein A (Sigma) and washed with lysis buffer (26). Samples were denatured by boiling in sample buffer (0.0625 M Tris-Cl [pH 6.8], 2% sodium dodecyl sulfate [SDS], 10% glycerol, 5% 2-mercaptoethanol) for 90 s prior to electrophoresis on 1.5-mm-thick SDS–10% polyacrylamide gels (Protogel; National Diagnostics, Inc.). Gels were fixed (40% methanol, 7% acetic acid), stained (0.025% Coomassie blue R-250), destained (7% acetic acid, 5% methanol) by standard methods (6), and soaked for 30 min in Fluoro-Hance (Research Products International). After drying, radioactive bands were detected with X-Omat AR5 film (Eastman Kodak Co.).

Light and scanning electron microscopy. CEF cultures were observed with a Zeiss IM35 inverted light microscope and photographed with a mounted Contax 137 automatic camera, using the 10× or 16× objective. For scanning electron microscopy, cells were cultured on glass coverslips for 3 to 4 days, washed with 0.1 M KPO_4, fixed with glutaraldehyde, stained with osmium tetroxide, processed as described previously (10), and analyzed with a Hitachi S-450 scanning electron microscope, emitting at 10 kV.

RESULTS

Effects on viral activities by mutagenesis of AUG codons in the RSV leader sequence. The strategy used for assessing the role of the ORFs in the 5′ leader sequence of RSV is depicted in Fig. 2. Essentially, permuted, linearized DNA constructs containing site-specific mutations were transfected into CEFs. Following uptake of the constructs, the viral long terminal repeat was able to direct viral RNA synthesis, which in turn served to provide both mRNA for viral protein synthesis and RNA genomes for the assembly of nascent virus that could subsequently infect other CEFs as detailed previously (50). Five assays were conducted to evaluate viral activities and the course of viral replication. Reverse transcriptase assays on samples of extracellular media (assay 1) provided a quantitative measure of the number of released viral particles; focus formation assays in soft agar (assay 2) provided a complementary insight into the ability of released particles to transform CEF cells; Northern (RNA) blot assays of intracellular viral RNA (assay 3) indicated both the relative concentrations and the sizes of RNA, which in turn gave the rate of accumulation of normal and transformation-defective (*td*) virus; immunoprecipitation analysis of the viral proteins Pr76^{gag} and pp60$^{v\text{-}src}$ (assay 4) indicated steady-state levels of viral protein synthesis; and micro-

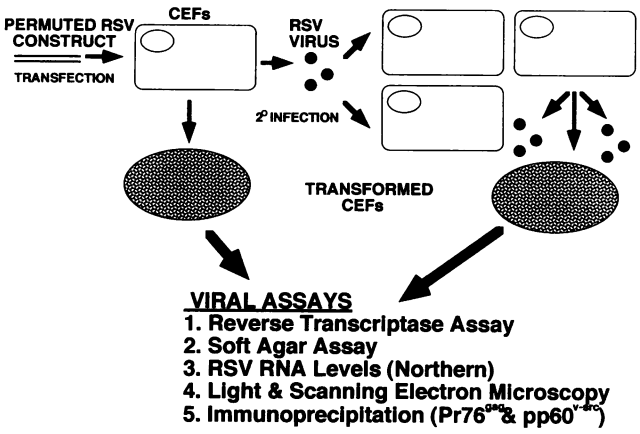

FIG. 2. Experimental strategy for examining ORF mutations. The linearized RSV mutant constructs are shown as the parallel lines which were transfected into CEFs. The upper horizontal pathway indicates that some transfected cells will produce viruses that are capable of infecting neighboring cells and establishing over time a plate of virus-infected cells, generally obvious by their transformed morphologies (shaded, rounded cell patterns). Assays of viral activity included reverse transcriptase activities and ability to form foci on soft agar. Assays for intracellular viral RNA and proteins and for morphological features by light and scanning electron microscopy established the presence and transforming ability of RSV in these cells.

scopic analysis of cellular morphology (assay 5) allowed assessments of cytopathology resulting from several of the viral mutants. Assays 1 and 2 were quantitative over a 10,000-fold range, assays 3 and 4 had about a 20-fold range, and assay 5 was qualitative. All experiments were repeated a minimum of five times.

Previously, we found that mutagenesis of the initiation codon of ORF1 (AUG→ACG) led to an attenuated rate of viral replication (50). We extended this analysis by inactivating ORF2 and ORF3 by mutagenesis of their AUG codons (designated AUG mutants; Fig. 1). Reverse transcriptase activities for the WT virus and the five constructs with mutations in one or more of the AUG codons in the leader sequence of RSV RNA are shown in Fig. 3A. The accumulation kinetics of mutants AUG1 and AUG2 and the double mutant AUG12 clearly show delays in the release of enzyme-containing virus. In contrast, mutants AUG3 and AUG123 did not release detectable levels of reverse transcriptase-containing particles, demonstrating the dominant phenotype of the AUG3 mutation. The delay in released reverse transcriptase activity from the AUG12-infected cells compared with the reverse transcriptase activities from the individual AUG1 and AUG2 mutations indicated an additive effect of the single mutations when linked together. In multiple transfection experiments, the reverse transcriptase kinetic curves of the AUG1 and AUG2 viruses reproducibly showed the first appearance of enzyme activity in the culture medium 7 to 10 days posttransfection, and the maximal level of radionucleotide incorporation was in the range of 2×10^3 to 5×10^3 cpm/μl of medium (Fig. 3A). The WT virus clearly spread at the most rapid rate. Steady-state levels of reverse transcriptase production were in the range of 2,000 to 3,000 cpm/μl of medium for all cultures that were able to release measurable levels of virus.

To ensure that the delayed onsets of reverse transcriptase activity were due to effects on the viral life cycle and not to some aspect of transfection or to either reversion of the mutant to WT or another suppression mutation, subsequent infections of fresh CEF cultures with virus-containing media collected from the initially transfected cultures were performed, and viral activity was monitored by reverse transcriptase (Fig. 3B) and focus formation (Table 1) assays. Equal titers of virus, measured by reverse transcriptase activity, were used in all reinfection experiments. The reverse transcriptase curves from reinfected cultures manifested shorter overall lags in the onset of reverse transcriptase activity, as a result of the difference between infection and transfection, but the delays in viral growth between the mutant and WT viruses were the same in transfected and infected cells (compare Fig. 3A and B), indicating that the delayed onset of particle release was not due to back or complementing mutations in the viral genome. The reverse transcriptase kinetics, summarized in Fig. 8, clearly demonstrate that mutations in the ORFs designed to prevent their translation impaired viral replication. Quite unexpectedly, mutations in AUG3 had the most pronounced effect even though all of our previous experiments indicated that this ORF is translationally inactive. These findings spurred further inquiry into the role of the ORFs in viral replication and pathology.

Effects of elongated ORFs on viral replication and gene expression. The sizes of the ORFs in the avian retroviruses are absolutely conserved even though the termination codons are variable in different viral strains (24). This conservation suggests that length may be important to ORF function. This hypothesis was tested by mutagenesis of the termination codons (TC mutants) to sense codons, with or without appropriate frameshifts to fuse the ORFs in frame. The strategy used for the AUG mutants was employed to construct the TC mutants. The lengths of the ORFs in the TC mutants changed from 7, 16, and 9 amino acids in the WT virus to 30 and 9 amino acids in TC1, 7 and 48 amino acids in TC2, and a single, 64-amino-acid ORF in TC1TC2. As shown in Fig. 3C and D and Table 1, mutants TC1, TC2, and TC3 produced reverse transcriptase-containing viruses and manifested transforming activity levels comparable to the WT level, whereas the TC1TC2 double mutant exhibited a substantially retarded release of reverse transcriptase-containing particles and was unable to transform CEFs. These data indicate that viruses with elongated leader ORFs of 30 to 48 codons behaved as WT. But when the RSV leader sequence contained a longer ORF of 62 codons behind an AUG codon with a translationally favorable context, the transforming capacity of the virus was reduced at least 10,000-fold below WT levels.

In all cases except the TC1TC2 double mutant, there was a correlation between focus formation ability and reverse transcriptase activity. The presence of enzymatic activity in the absence of transforming capability suggested that the RSV parental genome might have lost its *src* oncogene. This hypothesis could be tested by analysis of viral RNA following transfection to determine whether *td* virus was produced. RSV RNA accumulation in both the transfected and reinfected CEFs supported the observation that the three single TC mutations had little or no effect on virus production (Fig. 4A [TC1] and B [TC2 and TC3]). Although mutants TC1 and TC2 exhibited a slower rate of appearance of RSV RNA soon after transfection, their RNA levels achieved that of WT virus by day 12. Mutant TC3 accumulated viral RNA at the same rate as did WT virus. RSV RNA analysis from CEF cultures reinfected with mutant viruses revealed the same profiles of RNA accumulation as in the transfection experi-

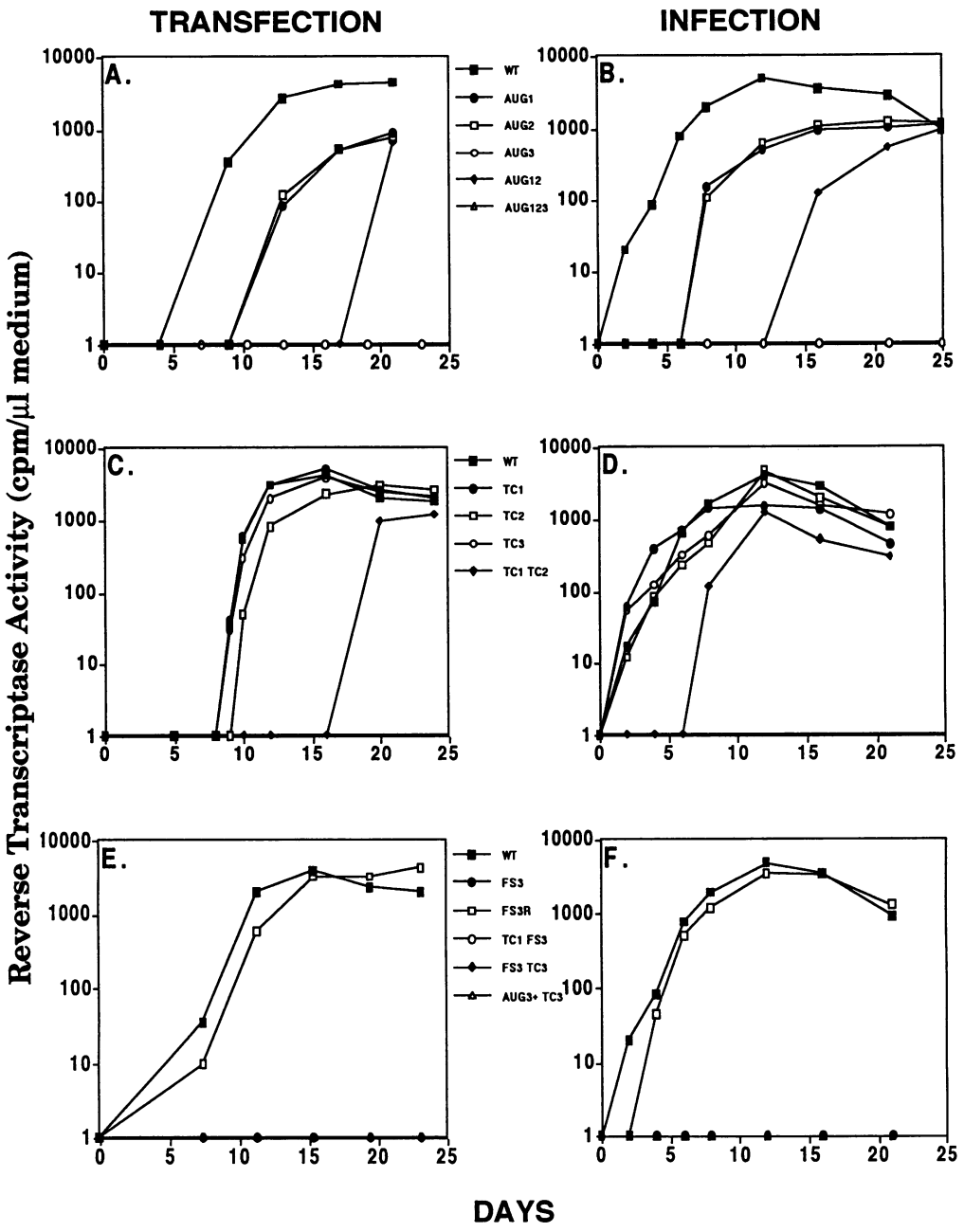

FIG. 3. Reverse transcriptase assays of mutant viruses. As described in Materials and Methods, RNA-dependent DNA polymerase activities were quantified in aliquots of media isolated following transfection and reinfection of CEFs. (A, C, and E) Enzyme activities following transfection of CEFs with the indicated DNA constructs; (B, D, and F) results of infection of CEFs with particles harvested 10 to 18 days posttransfection.

ments (41). RNA blots revealed that the three single termination codon mutants rapidly accumulated *td* virus (Fig. 4A, lanes c; Fig. 4B, lanes f and g). The transformed phenotype of cells infected with either TC1 or TC2 peaked at 15 or 8 days postinfection and thereafter regressed somewhat, presumably as a result of the accumulation of the observed *td* viruses lacking *src* (19). To ensure the identity of the *td* RNA species observed in our RNA analysis, we reprobed the blots with an *env*-specific probe (41). We found the same pattern of RNA species as with the full-size genomic RSV probe at late time points, confirming that the abundant low-molecular-weight species that migrated near the position of *src* mRNA on days 18 and 23 (Fig. 4A, lanes c and d) and on days 20 and 24 (Fig. 4B, lanes e to g) was *env* mRNA from *td* virus.

The patterns of viral protein synthesis in the mutants provided further insight into the effects of ORF mutations. Proteins from transfected cells were immunoprecipitated with either anti-RSV antibody, which precipates $Pr76^{gag}$ from cellular lysates, or anti-$pp60^{v\text{-}src}$ to determine the

TABLE 1. Cell transformation assay

Virus	FFU/ml[a]
WT	5.0×10^4
AUG1	2.0×10^4
AUG2	3.2×10^4
AUG3	55
AUG12	2.2×10^4[b]
AUG123	<10
TC1	2.0×10^4
TC2	2.0×10^4
TC3	2.5×10^4
TC12	<8
FS3	<8
FS3R	4.5×10^4
AUG3$^+$TC3	<10
TC1FS3	<8
FS3TC3	68

[a] Determined as described in the Materials and Methods.
[b] An eventual titer of 2.2×10^4 could be reached, but only after considerable time; AUG12 is a very slow virus.

effects on translation of unspliced and spliced RSV mRNA (Fig. 5). Pr76^{gag} was efficiently made in cells transfected with WT, AUG1, AUG2, TC1, TC2, and TC3 viruses but not in AUG3- and AUG123-transfected cells (Fig. 5A). In contrast, expression of pp60$^{v\text{-}src}$ (Fig. 5B) was somewhat higher in AUG1-, AUG2-, and TC3-transfected cells than in WT-infected cells. There was no evidence of *src* expression in AUG3-, AUG12-, and AUG123-transfected cells after 9 to 12 days of incubation, in keeping with the lack of other viral activities in these cells. These data are summarized in Fig. 8.

In contrast to the single TC mutants, the double termination codon mutant TC1TC2 produced undetectable levels of transforming activity (Table 1) and a delayed onset of replication (Fig. 3C and D). This mutant's reverse transcriptase profile resembled that of the AUG1 and AUG2 viruses, but the inability of the TC1TC2 virus to induce cellular transformation clearly distinguished it from the AUG mutants. Only the *td* RNA species accumulated after day 20 posttransfection (Fig. 4B, lanes e), whereas no full genomic or *src* RNA species ever appeared in cells transfected with the double mutant. This mutant virus apparently required a lag period of about a week before it could attain detectable levels of growth, by which time it had lost its oncogene and consequently its transforming ability. The levels of Pr76^{gag} made by this mutant were undetectable after 12 days, indicating a translational effect of the long upstream ORF on downstream initiation of protein synthesis.

Changing the AUG codon context of ORF3 abolished viral replication. The effects of elongating ORF1 into ORF2 and ORF3 in the TC1TC2 double mutant may have been due to disturbing ORF3 alone, which, as shown previously by the AUG3 mutant, was important to viral replication. To further probe the important aspects of ORF3 on viral propagation, we examined the effects of alterations in the ORF3 coding sequence. Five mutants were examined (summarized in Fig. 8). The first, FS3, had a frameshift mutation in the fourth nucleotide, which produced a translationally favorable initiation codon (35, 36) which was identical in nucleotide context to the AUG codon of ORF1 with respect to nucleotides −3 and +4 (Fig. 1) and which elongated ORF3 to 64 codons, which is about the length of the single ORF in the defective mutant TC1TC2 (62 codons) and equal to the length of ORF3 in mutant TC3, which showed a WT phenotype. The other four mutants were FS3R, which restored the translational context of AUG3 back to its normal context while maintaining the frameshift; FS3TC3, which maintained the frameshift but shortened the mutant reading frame of FS3 (64 codons) by a mutation in TC3 to 26 codons; TC1FS3, which was constructed to test whether a single 30-codon ORF upstream of ORF3 might affect its translation differently than when two shorter ORFs preceded it as with FS3; and AUG3$^+$TC3, which had (i) the translationally enhanced codon context for AUG3, (ii) the same extension of ORF3 as in the FS3 mutant, and (iii) nearly the same amino acid sequence at its amino-terminal end as the normal ORF3. With these mutants, we could distinguish effects of AUG initiation codon context, amino acid sequence of the encoded leader peptide, and ORF length.

Improving the AUG context of the elongated ORF3 from AUGA to AUGG resulted in severely defective viruses (FS3, FS3TC3, TC1FS3, and AUG3$^+$TC3) with respect to focus formation activity (Table 1), reverse transcriptase activity (Fig. 3E and F), and viral protein synthesis (Fig. 5). In contrast, FS3R, with the same, elongated length in ORF3 but with the original AUG3 codon context, had viral activities that were similar to those of WT virus. The activities of these mutants suggested that alterations of the fourth base of ORF3 had extreme consequences for viral replication. RNA blot analysis (Fig. 4A, lanes a and b) did not reveal any RSV-specific RNA species at any time posttransfection. DNA blot analysis on transfected CEFs indicated abundant levels of unintegrated viral fragments that carried the introduced mutation(s) up to 7 days posttransfection (41). Thus, the viral DNA was introduced into the cell successfully but was unable to support subsequent viral replication. This finding suggests that the change of the AUG codon context in position +4 of ORF3 was sufficient for the severely defective phenotype. Furthermore, results for mutants FS3R, AUG3$^+$TC3, and FS3TC3 together indicate that the defect in the FS3 mutation need not have been due either to the extension of ORF3 which overlapped with the *gag* coding region or to the alteration in the coding sequence of the ORF3 peptide. The TC1FS3 mutant had properties identical to those of the FS3 mutant, consistent with the previous observation that the TC1 mutation alone had no observable effect on viral replication.

Cellular senescence of FS3-infected CEFs. During the multiple transfection experiments used with the FS3 construct, individual cells appeared to be transformed (Fig. 6, arrowheads). Transformants were also observed upon reinfection of fresh CEFs with cell-free media from transfected cultures. Such transformants were few, scattered in the culture dish, and surrounded by lysed cell material that dissociated from the plate and floated in the medium (Fig. 6B, arrows). Transformed cells died 4 to 6 h after formation. Intriguingly, several hours after death, new transformants were located in the same area. These observations suggested that the virus in the infected cell was unable to replicate and spread but could induce a cytopathic effect.

To substantiate this observation, cell morphology was examined by scanning electron microscopy. Figure 7 shows representative micrographs of CEFs infected with WT RSV (panels 1 and 2) and with the two mutants FS3 and TC1FS3 (panels 3 to 6). Whereas cells infected with WT RSV expressed the distinct surface morphology (2, 3, 55) of a transformed fibroblast (panels 1 and 2, T), cultures infected with FS3 and TC1FS3 looked like uninfected fibroblasts

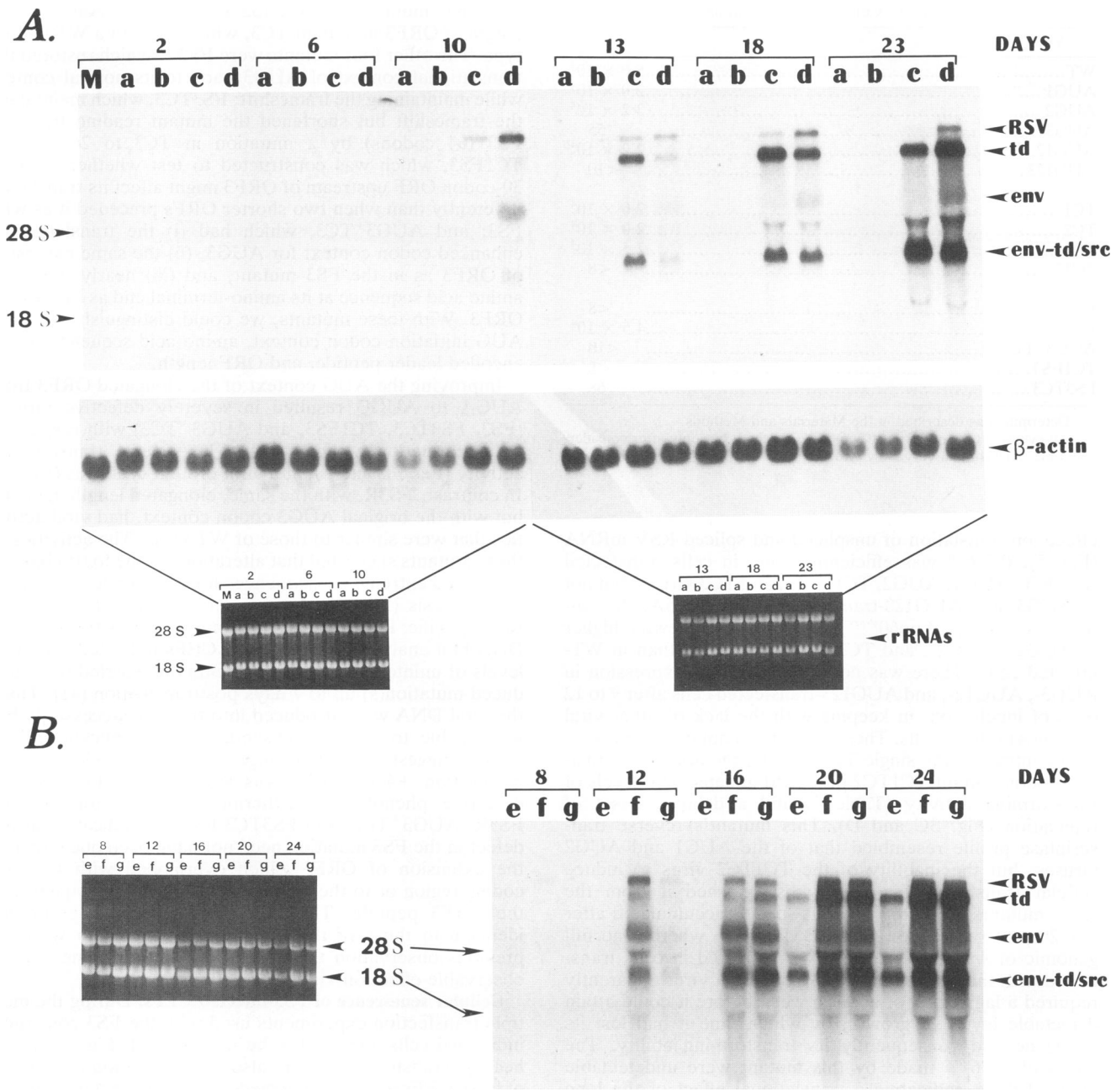

FIG. 4. Northern analysis of RSV RNAs in transfected CEFs. Autoradiograms of the RNA profiles are shown from samples from transfected cells that were separated on 1.2% agarose gels containing formaldehyde. (A) The upper panel shows results for mock-transfected CEFs (lane M) and CEFs transfected with FS3, TC1FS3, TC1, and WT RSV (lanes a to d, respectively). The lower panel shows both the original gels in the upper panel stained with ethidium bromide to show 18S and 28S rRNA levels and the same filters blotted with a β-actin mRNA probe for internal standardization of the viral RNA signals. (B) Viral RNA patterns from cells transfected with mutant constructs TC1TC2, TC3, and TC2 (lanes e to g, respectively). The panel at the bottom left shows the ethidium bromide staining of the rRNAs from the samples in the upper panel. The number above each set of lanes corresponds to the number of days after transfection that the samples were harvested for analysis. Positions of the full-size genomic RNA (RSV), *td* genomic RNA (td), *env* mRNA (env), *src* mRNA, and *env*(*td*) mRNA (which comigrates with the *src* mRNA) (env-td/src) are designated at the right.

(panels 3 and 5, F). Only after systematic searches were individual transformants identified from the two mutants (panels 4 and 6, T); pairs of transformants which might have suggested associated daughter cells undergoing mitosis were never observed. The surface morphology was different than that of WT RSV transformants. The cells infected with mutant viruses expressed a phenotype which lacked the normal rich and dense network of microvilli and extended philopodia (panels 1 and 2, large arrowheads) and had short and loosely scattered microvilli (panels 4 and 6, small

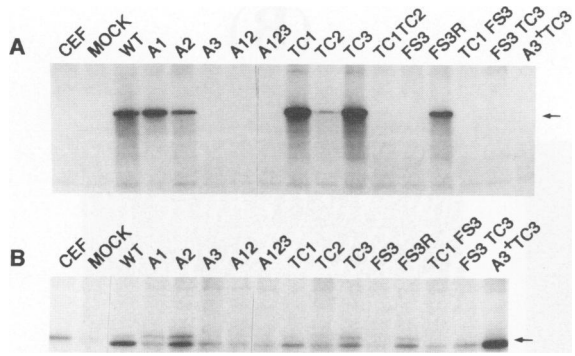

FIG. 5. Analysis of viral protein in cells infected with mutant viruses. Cell lysates were obtained from [^{35}S]Met-labeled cells transfected 9 (A) and 12 (B) days prior with the indicated mutants. Proteins were immunoprecipitated as described in Methods and Materials and separated on 10% polyacrylamide gels. The viruses are labeled above the lanes. A molecular weight standard was run in each gel (not shown). (A) Proteins precipitated with anti-RSV antiserum. The position of Pr76^{gag} is noted by the arrow at the right. (B) Protein precipitated with a pp60$^{v\text{-}src}$ monoclonal antibody. The position of pp60$^{v\text{-}src}$ is noted by the arrow at the right; both bands are forms of pp60$^{v\text{-}src}$ (58).

arrowheads). Furthermore, these putative mutant transformants showed a very low abundance of ruffles relative to the WT transformants. The limited number of surface membrane structures might be indicative of abortive efforts for cell division which resulted in subsequent senescence.

DISCUSSION

The results presented in this report support our hypothesis that the ORFs in the leader RNA sequences of avian retroviruses are translated and important for viral replication. Inactivation of AUG1 and AUG2 individually or together delayed and/or reduced the levels of viral RNA synthesis. Mutagenesis of AUG3 eliminated viral replication almost completely. Alteration of the context of the ORF3 initiation codon had a similar debilitating effect on the retrovirus. Extensions of ORFs in some circumstances suppressed viral propagation. The effects of the ORF mutagenesis experiments are summarized in Fig. 8. Mutations in the leader RNA sequence could have had effects on reverse transcription-proviral insertion, viral RNA translation, and/or viral RNA packaging. The following two hypotheses could account for our observations that mutations in the leader RNA interferred with viral replication. (i) Mutations in the leader ORFs may affect translation of *gag*, *gag-pol*, *env*, and *src* mRNAs. (ii) ORF mutations may alter RNA secondary structural motifs required for reverse transcription and/or packaging of the viral RNA.

Hypothesis 1: the ORF mutations affect synthesis of RSV proteins. Mutations in AUG1 and AUG2 had relatively small effects, generally retarding the rate of viral propagation, whereas the AUG12 mutant caused a more pronounced reduction in the ability of RSV to replicate (Fig. 3) and reduced the synthesis of viral proteins (Fig. 5). These results are in accord with previous evidence which indicated that the first two ORFs are translated (50). The presence of at least one of the first two ORFs appears to be important for improving translational efficiency of the *gag*, *pol*, and *env* coding regions by facilitating ribosomal movement along the unusually long 5′ leader region or for altering the folded structure of the viral RNA to facilitate viral RNA packaging. The major effects following alteration of ORFs that we observed differ from those reported by Donzé and Spahr (17). In our experiments, mutagenesis of AUG3 in mutants AUG3 and AUG123 completely suppressed viral replication, as measured by reverse transcriptase activity and spread of cellular transformation (Fig. 3 and 8), whereas their equivalent mutants, pAM3 and pAMuP, actually enhanced viral replication and delayed transformation only in the case of pAM3. Additionally, we found that mutation of AUG2 in mutants AUG2 and AUG12 delayed the onset of reverse transcriptase activity by 1 to 2 weeks and reduced its level nearly 10-fold, whereas the equivalent mutants in the Donzé and Spahr study, pAM2 and pAM1AM2, showed no reduction in activity. Since their assays were conducted at a single time, in contrast to our measurements over 2 weeks, and since the site-specific mutations altered different nucleotides in their mutants, the cause of the differences in results cannot be completely resolved.

The role of ORF3 is perplexing. All of our previous assays of translational activity suggested that it is relatively silent (48–50), yet mutation of its initiation codon (AUG3) or change in the context of its AUG codon (AUG3$^+$ and the FS3 mutant series) are all compatible with ORF3 being translationally active. Nevertheless, the effects of the mutations in ORF3 can be rationalized by consideration of its location in the leader. ORF3 is situated in a particularly metastable region of RNA secondary structure that overlaps a region required for RNA packaging and virion formation; ORF3 is also proximal to the AUG initiation codon for all of the structural proteins of the virus (23). Accordingly, high rates of ORF3 translation in the AUG3$^+$ and FS3 mutants may prohibit efficient *gag*, *gag-pol*, and *env* protein synthesis, by converting scanning subunits into complete ribosomes before they encounter the fourth AUG codon, thereby inhibiting viral propagation. An alternative hypothesis (17) that the effects of the FS3 mutation were due to the encoded polypeptide in the elongated ORF3 is unlikely. Although the FS3 mutation changed the eight amino-proximal amino acids (excluding the N-terminal methionine) of ORF3, mutant FS3R, which differed from FS3 at only one site (Thr to Ala in the second residue), had the WT phenotype even though the remaining 63 amino acids were the same. Moreover, the AUG3$^+$TC3 mutant with an enhanced AUG3 codon context but the same amino-terminal residues as in the normal ORF3 was as inactive as the FS3 mutants. Thus, comparison of the FS3, FS3R, and AUG3$^+$TC3 mutants as well as examination of ORF3 sequences in other replication-competent avian retroviruses (24, 28) are consistent with a model wherein the effects of the FS3 mutation were due to enhanced translation of ORF3 that reduced translation of the major viral proteins which initiate at the fourth AUG codon. In the same fashion, the FS3 mutation should reduce translation of the spliced *env* mRNA because the termination codon of the elongated ORF3 resides downstream from the *env* initiation codon (Fig. 1).

Altered translation may explain potential lethal effects of the FS3 mutation. In the spliced *src* mRNA, the elongated ORF3 terminates within the fourth upstream ORF, which is normally translated (30). Moreover, just as nonsense codons in the *gag* gene can destabilize unspliced RSV mRNA (7), the overlap of the FS3 ORF into the *gag* coding sequences could also destabilize the unspliced mRNA by the same mechanisms. Accordingly, our model suggests that translation through ORF3 of mutant FS3 suppresses *gag* and *env* translation but may enhance *src* protein synthesis to cyto-

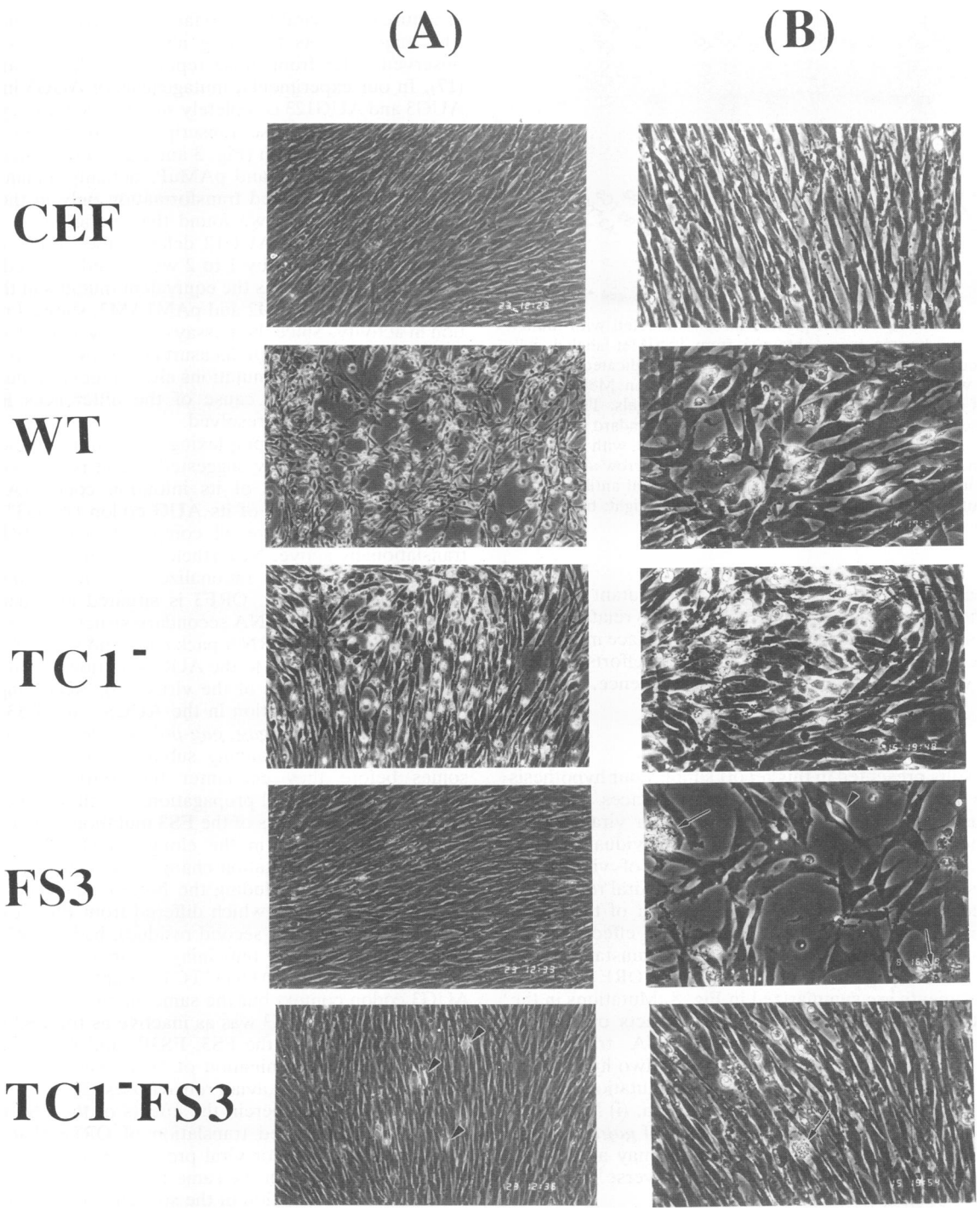

FIG. 6. Light micrographs of uninfected CEFs (CEF) and CEFs infected with WT or mutant (TC1, FS3, and TC1FS3) virus. Micrographs of tissue-cultured cells were obtained 18 days posttransfection (A, ×90 magnification) and 14 days postinfection (B, ×145 magnification). The micrographs of cells harboring WT and TC1 viruses clearly show multiple transformed CEFs. The pictures of FS3- and TC1FS3-infected cells show individual transformed CEFs (arrowheads) and senescent cells (arrows) located at areas previously occupied by transformed CEFs.

toxic levels (58). We are currently examining this possibility (52, 58).

From the foregoing considerations, destruction of AUG3 to eliminate the normally translationally silent ORF3 was not expected to have any effect on viral protein synthesis. However, alteration of AUG3 inactivated the virus. As explained below, mutants with the AUG3 mutation may be impaired as the result of an inability to productively encapsidate the viral RNA.

Extensions of the ORFs could affect either translation of viral proteins or packaging. The TC1 and TC2 mutations did not appear to affect other important *cis*-acting sequences in

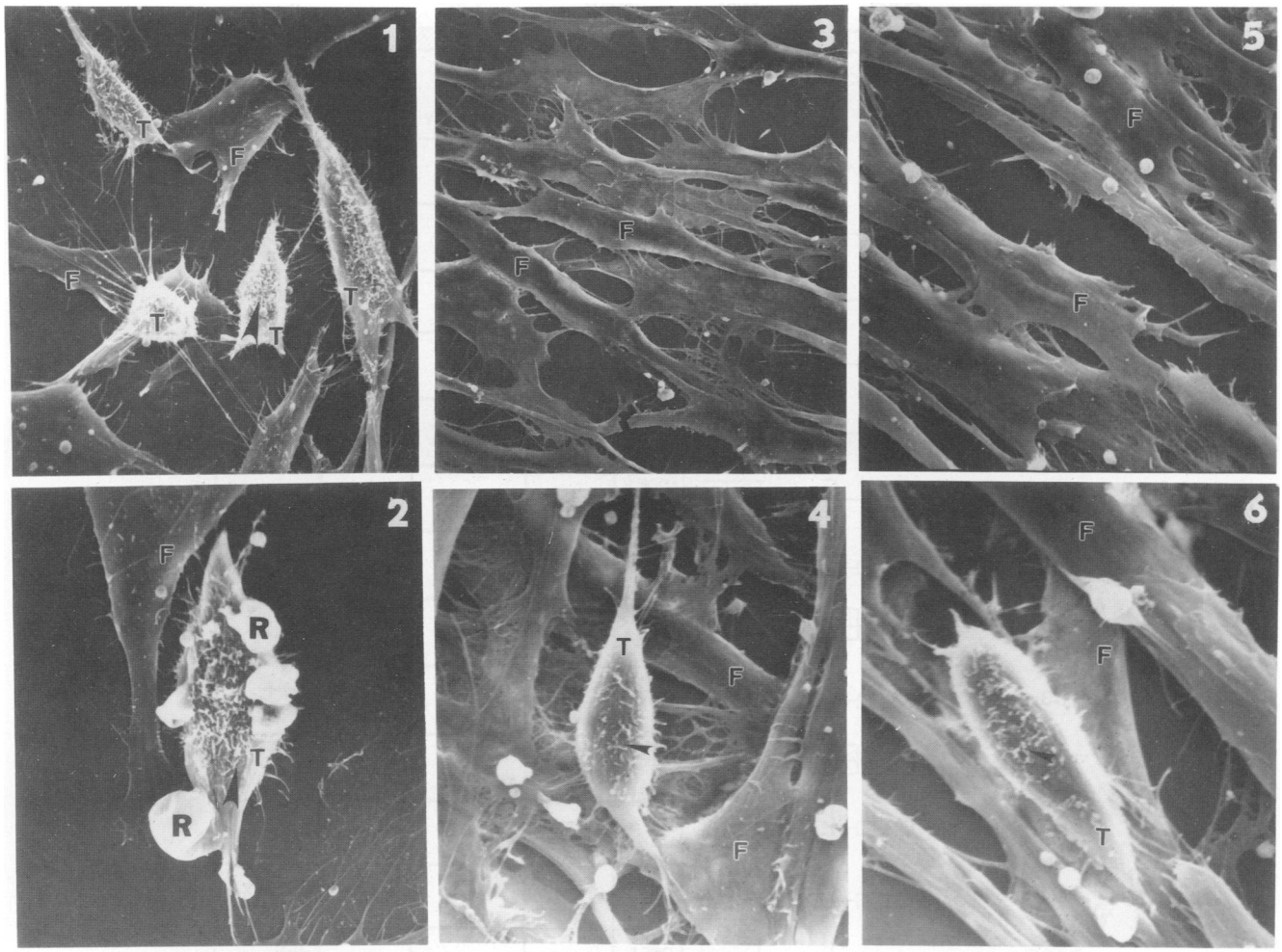

FIG. 7. Scanning electron micrographs of CEFs infected with WT RSV (1 and 2), FS3 (3 and 4), and TC1FS3 (5 and 6). Cell cultures were prepared for microscopy at 12 days postinfection. Panel 1 shows four transformed CEFs (T) and neighboring uninfected fibroblasts (F); panels 3 and 5 shows normal CEF cell layers (F); panels 2, 4, and 6 show individual transformed CEFs (T) and underlying normal fibroblasts (F). Networks of microvilli are indicated by arrowheads (large arrowheads, rich and dense networks; small arrowheads, poor and loose networks). Two individual ruffles of the transformed cell in panel 2 are labeled R. Magnifications: 1, ×800; 2, ×1,400; 3, ×1,000; 4, ×2,000; 5, ×1,200; 6, ×2,400.

the RSV leader, since neither mutation had a substantial effect on virus propagation. However, replication of the double mutant (TC1TC2) was profoundly retarded. These results suggest that if ORF 1 exceeds a threshold length, between 48 and 62 codons, ribosomes would no longer be able to reinitiate at the initiation codon for the *gag* gene. The proposal that threshold lengths of nascent polypeptides longer than 50 to 60 amino acids may lead to translational termination is supported by the effects of upstream ORFs on polycistronic mRNAs in plant protoplasts (20) and the mode of translational regulation of tubulin protein synthesis in animal cells (21). Coincidentally, the average ribosome-protected length of nascent peptide sequence is about 50 amino acids (39), suggesting that once the nascent peptide protrudes from the 80S ribosome, further reinitiation of translation is inhibited. Thus, the data for the TC mutants further support our previous conclusion (50) that ORF1 is translated in vivo.

Additionally, the data support the hypothesis that either translation of elongated ORFs or enhanced translation of an ORF that overlaps the *gag* coding region interferes with translation of the major viral proteins. These conclusions are in accord with our previous findings (48–50) and are further developed in the accompanying report (42), wherein the intrinsic translational efficiencies of the mutant viral RNAs are examined.

Hypothesis 2: the ORF mutations may affect RNA conformations required for viral replication. Reverse transcription and encapsidation of retroviral RNA require recognizable motifs in the leader sequence (1, 4, 5, 8, 15, 23, 34, 44, 51). Following infection, viral RNA is reverse transcribed by reverse transcriptase, which requires a specific RNA conformation around the primer binding site, the PBL loop (23). Alteration of this structure impairs provirus synthesis and virus spread (1, 14). The AUG2 mutation is in the PBL structure and may subtly alter the folded pattern of the bases in a manner similar to that observed by Cobrinik et al. (14). Since the AUG codon of ORF1 is outside the PBL structure (23), it is less likely that the effect of the AUG1 mutation interferes in this manner with reverse transcription. In cells

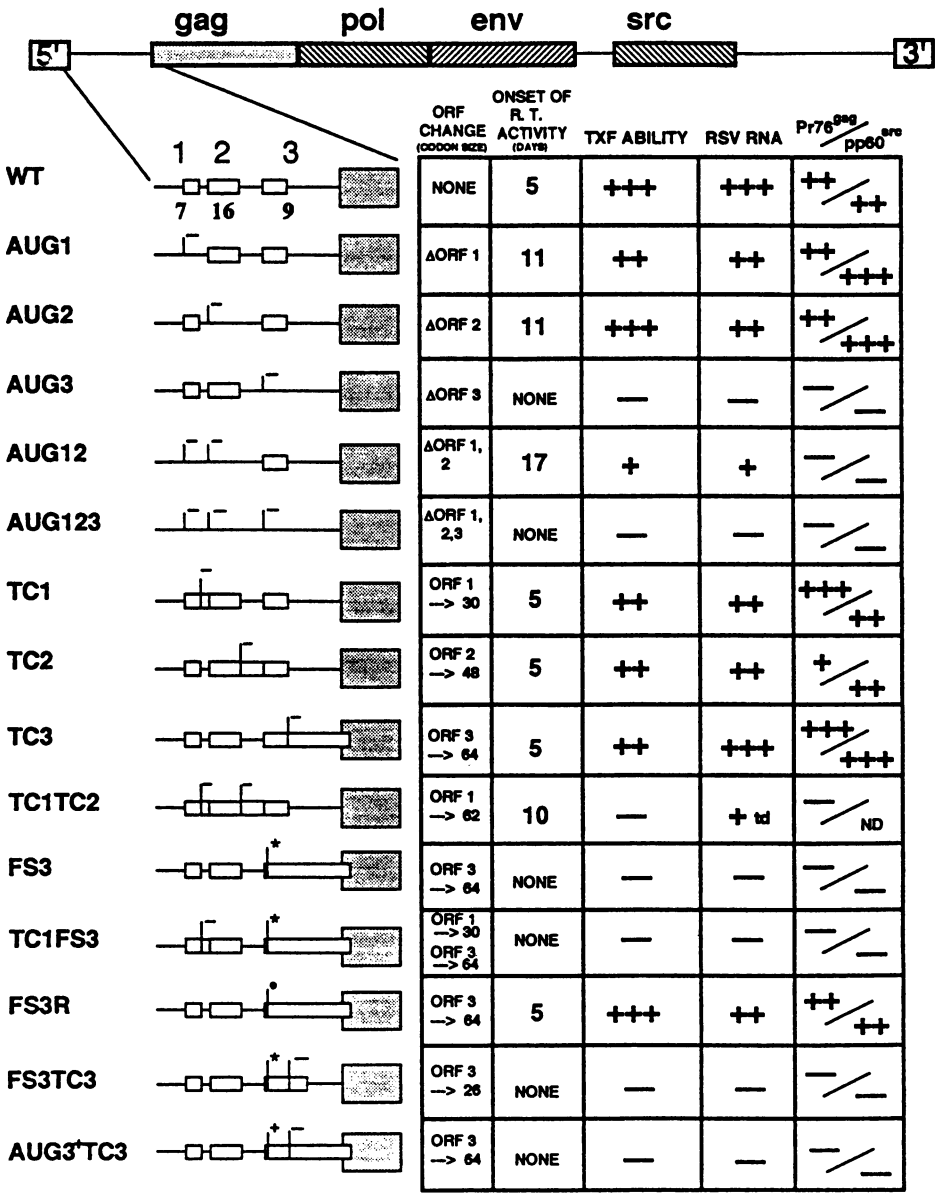

FIG. 8. Summary of RSV mutant clones and phenotypes. The RSV genomic RNA is shown at the top. Its four genes are shown as large boxes, and ORF1 to ORF3 in the 5′ leader sequence are shown in the expanded segments below the map of the entire virus. The ORFs are indicated by the numbers above the WT diagram, and the numbers of encoded amino acids are indicated below the ORFs. Sites of mutations are indicated by vertical lines above the maps. Alterations of initiation or termination codons are indicated by dashes, the frameshifts in the FS3 mutants are indicated by asterisks, and the base substitution in the +4 position of the AUG3 codon is indicated by a plus sign. The tabulation indicates changes in ORF lengths (ΔORF), the number of days posttransfection when reverse transcriptase (R.T.) activity was first noted (Fig. 3), the relative level of transformation (TXF) taken from Table 1, the levels of intracellular retroviral RNA detected by Northern blot analysis (Fig. 4 and reference 52), and the levels of steady-state $Pr76^{gag}$ and $pp60^{v\text{-}src}$ detected by immunoprecipitation (Fig. 5). Symbols for the transformation assay: +++, >3 × 10^4 FFU/ml; ++, 100 to 3 × 10^4 FFU/ml; +, 10 to 100 FFU/ml; −, 10 FFU/ml.

producing virus, full-length retroviral RNA molecules continually enter pools to become either templates for protein synthesis or substrates for encapsidation. We hypothesize that a biochemical equilibrium mediated by the $Pr76^{gag}$ concentration determines the pool into which an RNA goes after leaving the nucleus. A simple model is that competition between ribosome formation at the *gag* initiation codon and *gag* polyprotein association with the Ψ packaging motif on the viral RNA determines the equilibrium. Accordingly, when an RNA enters the polysome pool, the increased production of *gag* protein tends to shift the equilibrium to packaging by raising the probability that a $Pr76^{gag}$ protein will bind to the leader and prevent further ribosomal subunit scanning. Likewise, association of *gag* proteins with RNA during packaging and subsequent virus export will lower the intracellular $Pr76^{gag}$ concentration, thereby shifting the equilibrium back so that newly synthesized RNA would associate with ribosomes. This equilibrium could be disrupted by

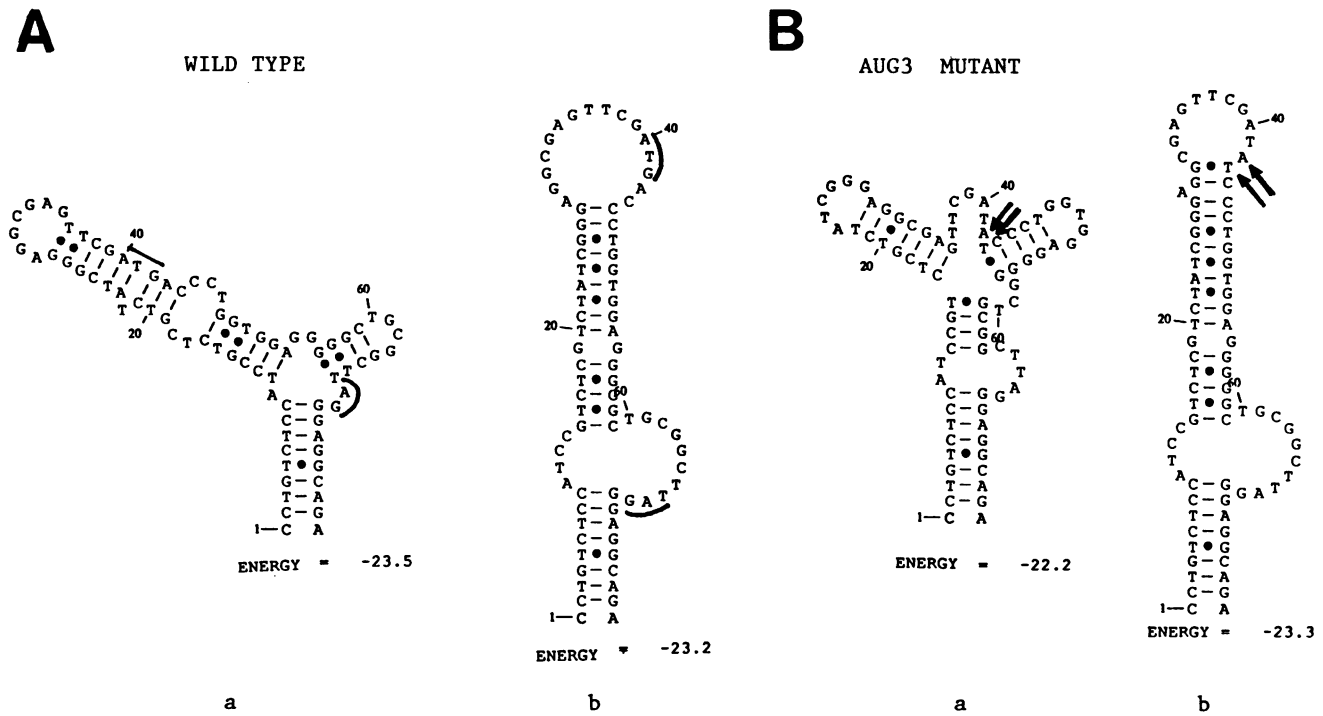

FIG. 9. Computer-generated RNA secondary structures (24) of the ORF3 packaging site region of RSV RNA, nucleotides 159 to 236 in the SR-A(SF) strain. Nucleotide 1 in the structures corresponds to residue 159. (A) Alternative structures of this region for the WT sequence, with the initiation and termination codons overlined. The ΔG of conformations a and b are −23.5 and −23.2 kcal (1 kcal = 1.484 kJ)/mol, respectively. (B) Comparable structures in the AUG3 RNA (arrows indicate the mutations). Note that the equilibrium is shifted in the opposite direction in AUG3 RNA compared with the WT RNA and that the multiple-loop structure a in the AUG3 mutant has a conformation different from that of structure a in the WT sequence.

either interference with Pr76^{gag} protein synthesis or alteration of the motifs of RNA structure recognized by the packaging proteins.

Selection of viral RNA for packaging requires a particular sequence in the leader RNA (4, 5, 8, 15, 27, 34, 38, 44, 51) that can form alternative conformations of folded RNA (23) (Fig. 9). ORF3 overlaps this metastable sequence required for efficient RNA packaging (51), and mutations in this ORF may inhibit encapsidation by altering required secondary structure in its vicinity. As shown in Fig. 9, the AUG3 mutation alters both the equilibrium of structures a and b and the folded pattern of structure a. In the model presented above, the ΔG values indicate that the RNA in the AUG3 mutant would assume conformation b four times more frequently than it would in the WT virus. Thus, though ample *gag* protein would be made in AUG3-transfected cells, the structure of the AUG3 RNA may not be as able to assume a folded structure compatible for packaging. Preliminary observations on the intracellular level of Pr76^{gag} polyprotein synthesis in AUG3 mutant-transfected cells support this hypothesis (42). By this model, augmented translation through ORF3 in the encapsidation recognition region, by complete 80S ribosomes rather than by scanning ribosomal subunits, might interfere with the process of Pr76^{gag} binding to the RSV RNA and the encapsidation process (8, 18, 35, 45). Our model parallels a hypothesis that ribosome binding to RNA and translation may affect encapsidation of hepadnavirus RNA (11, 43). This model has the further attractive feature of reconciling a recent report which conflicts with our observations. Donzé and Spahr (17) have suggested that ORF3 is translationally active and that the encoded peptide participates in some step, other than the packaging reaction, required in the viral life cycle. However, their ORF3 mutants pAM3^{185} and pAM3^{224} (17) contradict this conclusion, as do all of our findings with our ORF3 mutants reported here, the translational effects of the ORF3 mutants (42), and ribosome binding studies which indicate that ORF3 is translated at most to only a small extent (48, 50). All of their critical changes in ORF3 were interpreted in terms of amino acid changes in the peptide without any apparent consideration of effects on RNA structure. Alteration in RNA folding could be the key to the incapacitation of the mutants in these studies of leader function. Relatively small alterations of RNA structure in other regions of the RSV and other retroviral leader RNAs have been shown to have major consequences (1, 14, 27).

The phenomenon of cell transformation followed by early cell death described in this work is unprecedented. Subgroup A avian retroviruses usually do not induce cytopathic effects. In the cases where cytotoxicity has been observed in cells infected with certain other subgroups of avian retroviruses, senescence has been attributed to superinfection phenomena (56). A delay in the acquisition of superinfection resistance seems to lead to massive second-round infection and transient accumulation of large amounts of unintegrated viral DNA whose dose must have been lethal. Another hypothesis proposes linkage of the receptor (specific for subgroup B viruses) with cell metabolism and the triggering of cytopathic phenomena by the interaction of the receptor with variant *env* glycoproteins (16). Neither of these hypotheses explains our results. We observed transformation of host cells prior to their senescence, indicating translation of

the spliced *src* mRNA. Possibly, $pp60^{v\text{-}src}$ expression from a virus that cannot be assembled and mature efficiently, because of either low levels of *gag*, *gag-pol*, and/or *env* proteins or a defect in packaging initiation due to translation through the packaging site, might lead to cytopathic effects. A more attractive hypothesis is that the FS3 mutation affects $pp60^{v\text{-}src}$ synthesis from the spliced *src* mRNA, thereby raising the concentration of the oncoprotein to cytotoxic levels (54). We are currently investigating this possibility (58).

In summary, we have provided an extended analysis of the role of the ORFs in the RSV leader RNA. Our data suggest that the viral life cycle is sensitive to the presence of the three ORFs which may be involved in the partitioning of RNA into polysomal and packaging pools.

ACKNOWLEDGMENTS

We thank R. Petersen and S. Belzer for preparing primary CEFs from embryonated eggs; R. Petersen and T. Holm for help in mutagenizing the stop codon of ORF1; J. Wehner for assistance during the construction of mutants FS3 and TC1; R. Kuehn for assistance with the scanning electron microscopy; D. Johnson for computer assistance in RNA folding; J. Wills (Pennsylvania State University) for the gift of the anti-RSV antiserum; and L. Wu, J. Essner, S. Fahrenkrug, R. Iwan, and the J. Wills laboratory for helpful conversations during the course of this work.

This project was supported by NIH (RO1 CA 43881) and the American Cancer Society (NP-790) grants to P.B.H. and by funds from the Aristotle Onassis Fellowship Fund and a University of Minnesota Graduate School fellowship to A.M.

REFERENCES

1. **Aiyar, A., D. Cobrinik, Z. Ge, H.-J. Kung, and J. Leis.** 1992. Interaction between retroviral U5 RNA and the TΨC loop of the $tRNA^{Trp}$ primer is required for efficient initiation of reverse transcription. J. Virol. **66**:2464–2472.
2. **Allred, L. E., and K. R. Porter.** 1979. Morphology of normal and transformed cells. *In* R. O. Hynes (ed.), Surfaces of normal and malignant cells. John Wiley & Sons, New York.
3. **Ambros, V. R., L. B. Chen, and J. M. Buchanan.** 1975. Surface ruffles as markers for studies of cell transformation by Rous sarcoma virus. Proc. Natl. Acad. Sci. USA **72**:3144–3148.
4. **Anderson, D. J., P. Lee, K. L. Levine, J. Sang, S. A. Shah, O. O. Yang, P. R. Shank, and M. L. Linial.** 1992. Molecular cloning and characterization of the RNA packaging defective retrovirus SE21Q1b. J. Virol. **66**:204–216.
5. **Aronoff, R., and M. Linial.** 1991. Specificity of retroviral RNA packaging. J. Virol. **65**:71–80.
6. **Ausubel, F. M., R. Brent, R. E. Kingston, D. D. Moore, J. A. Smith, J. G. Seidman, and K. Struhl (ed.).** 1987. Current protocols in molecular biology. John Wiley and Sons, New York.
7. **Barker, G. F., and K. Beemon.** 1991. Nonsense codons within the Rous sarcoma virus *gag* gene decrease the stability of unspliced viral RNA. Mol. Cell. Biol. **11**:2760–2768.
8. **Bieth, E., C. Gabus, and J.-L. Darlix.** 1990. A study of the dimer formation of Rous sarcoma virus RNA and of its effect on viral protein synthesis *in vitro*. Nucleic Acids Res. **18**:119–127.
9. **Bizub, D., R. A. Katz, and A. M. Skalka.** 1984. Nucleotide sequence of noncoding regions in Rous-associated virus-2: comparisons delineate conserved regions important in replication and oncogenesis. J. Virol. **49**:557–565.
10. **Boyde, A., R. A. Weiss, and P. Vesely.** 1972. Scanning electron microscopy of cells in culture. Exp. Cell Res. **71**:313–324.
11. **Chang, L.-J., D. Ganem, and H. E. Varmus.** 1990. Mechanism of translation of the hepdnaviral polymerase (P) gene. Proc. Natl. Acad. Sci. USA **87**:5158–5162.
12. **Chomczynski, P., and N. Sacchi.** 1987. Single-step method of RNA isolation by acid guanidinium thiocyanate-phenol-chloroform extraction. Anal. Biochem. **162**:156–159.
13. **Cleveland, D. W., M. A. Lopata, R. J. MacDonald, N. J. Cowan, W. J. Rutter, and M. W. Kirschner.** 1980. Number and evolutionary conservation of α- and β-tubulin and cytoplasmic β- and γ-actin genes using specific cloned cDNA probes. Cell **20**:95–105.
14. **Cobrinik, D., L. Soskey, and J. Leis.** 1988. A retroviral RNA secondary structure required for efficient initiation of reverse transcription. J. Virol. **62**:3622–3630.
15. **Darlix, J.-L.** 1986. Control of Rous sarcoma virus RNA translation and packaging by the 5′ and 3′ untranslated sequences. J. Mol. Biol. **189**:421–434.
16. **Dorner, A. J., and J. M. Coffin.** 1986. Determinants for receptor interaction and cell killing on the avian retrovirus glycoprotein gp85. Cell **45**:365–374.
17. **Donzé, O., and P.-F. Spahr.** 1992. Role of the open reading frames of Rous sarcoma virus leader RNA in translation and genome packaging. EMBO J. **11**:3747–3757.
18. **Dupraz, P., and P.-F. Spahr.** 1992. Specificity of Rous sarcoma virus nucleocapsid protein in genomic RNA packaging. J. Virol. **66**:4662–4670.
19. **Estis, L. F., and H. M. Temin.** 1979. Suppression of multiplication of avian sarcoma virus by rapid spread of transformation-defective virus of the same subgroup. J. Virol. **31**:389–397.
20. **Futterer, J., and T. Hohn.** 1992. The role of an upstream open reading frame in the translation of polycistronic mRNAs in plant cells. Nucleic Acids Res. **20**:3851–3857.
21. **Gay, D. A., S. S. Sisodia, and D. W. Cleveland.** 1989. Autoregulatory control of β-tubulin mRNA stability is linked to translation elongation. Proc. Natl. Acad. Sci. USA **86**:5763–5767.
22. **Goff, S., P. Traktman, and D. Baltimore.** 1981. Isolation and properties of Moloney murine leukemia virus mutants: use of a rapid assay for release of virion reverse transcriptase. J. Virol. **38**:239–248.
23. **Hackett, P. B., D. P. Johnson, M. W. Dalton, and R. B. Petersen.** 1991. Phylogenetic and physical analysis of the 5′ leader RNA sequences of avian retroviruses. Nucleic Acids Res. **19**:6929–6934.
24. **Hackett, P. B., R. B. Petersen, C. H. Hensel, F. Albericio, S. I. Gunderson, A. C. Palmenberg, and G. Barany.** 1986. Synthesis *in vitro* of a seven amino acid peptide encoded in the leader RNA of Rous sarcoma virus. J. Mol. Biol. **190**:45–57.
25. **Hackett, P. B., R. Swanstrom, H. E. Varmus, and J. M. Bishop.** 1982. The leader sequence of the subgenomic mRNAs of Rous sarcoma virus is approximately 390 nucleotides. J. Virol. **41**:527–534.
26. **Harlow, E., and D. Lane.** 1988. Antibodies: a laboratory manual. Cold Spring Harbor Laboratory, Cold Spring Harbor, N.Y.
27. **Harrison, G. P., and A. M. L. Lever.** 1992. The human immunodeficiency virus type 1 packaging signal and major splice donor region have a conserved stable secondary structure. J. Virol. **66**:4144–4153.
28. **Hensel, C. H.** 1987. Influences of RNA structure on initiation of protein synthesis on Rous sarcoma virus RNA. Ph.D. thesis. University of Minnesota, St. Paul.
29. **Hensel, C. H., R. B. Petersen, and P. B. Hackett.** 1989. Effects of alterations in the leader sequence of Rous sarcoma virus RNA on initiation of translation. J. Virol. **63**:4986–4990.
30. **Hughes, S., K. Mellstrom, E. Kosik, F. Tamanoi, and J. Brugge.** 1984. Mutation of a termination codon affects *src* initiation. Mol. Cell. Biol. **4**:1738–1746.
31. **Hunter, E.** 1979. Biological techniques for avian sarcoma viruses. Methods Enzymol. **38**:379–393.
32. **Johansen, H., D. Schumperli, and M. Rosenberg.** 1984. Affecting gene expression by altering the length and sequence of the 5′ leader. Proc. Natl. Acad. Sci. USA **81**:7698–7702.
33. **Katz, R. A., B. R. Cullen, R. Malavarca, and A. M. Skalka.** 1986. Role of the avian retrovirus mRNA leader in expression: evidence for novel translational control. Mol. Cell. Biol. **6**:372–379.
34. **Katz, R. A., R. W. Terry, and A. M. Skalka.** 1986. A conserved *cis*-acting sequence in the 5′ leader of avian sarcoma virus RNA is required for packaging. J. Virol. **59**:163–167.
35. **Kozak, M.** 1987. At least six nucleotides preceding the AUG

initiator codon enhance translation in mammalian cells. J. Mol. Biol. **196**:947–950.
36. **Kozak, M.** 1987. An analysis of 5′-noncoding sequences from 699 vertebrate messenger RNAs. Nucleic Acids Res. **15**:8125–8148.
37. **Kozak, M.** 1992. A consideration of alternative models for the initiation of translation in eukaryotes. Crit. Rev. Biochem. Mol. Biol. **27**:385–402.
38. **Linial, M., and D. Blair.** 1982. Genetics of retroviruses, p. 649–783. *In* R. Weiss, N. Teich, H. Varmus, and J. Coffin (ed.), RNA tumor viruses. Cold Spring Harbor Laboratory, Cold Spring Harbor, N.Y.
39. **Malkin, L. I., and A. Rich.** 1967. Partial resistance of nascent polypeptide chains to proteolytic digestion due to ribosomal shielding. J. Mol. Biol. **26**:329–346.
40. **Moustakas, A.** 1991. Genetic analysis of the three short open reading frames of the Rous sarcoma virus leader RNA sequence. Ph.D. thesis. University of Minnesota, St. Paul.
41. **Moustakas, A., and T. Sonstegard.** Unpublished data.
42. **Moustakas, A., T. S. Sonstegard, and P. B. Hackett.** 1993. Effects of the open reading frames in the Rous sarcoma virus leader RNA on translation. J. Virol. **67**:4350–4357.
43. **Nassal, M., M. Junker-Niepmann, and H. Schaller.** 1990. Translational inactivation of RNA function: discrimination against a subset of genomic transcripts during HBV nucleocapsid assembly. Cell **63**:1357–1363.
44. **Nishizawa, M., T. Koyama, and S. Kawai.** 1985. Unusual features of the leader sequence of Rous sarcoma virus packaging mutant TK15. J. Virol. **55**:881–885.
45. **Oertle, S., and P.-F. Spahr.** 1990. Role of the *gag* polyprotein precursor in packaging and maturation of Rous sarcoma virus genomic RNA. J. Virol. **64**:5757–5763.
46. **Olsen, J. C., and R. Swanstrom.** 1985. A new pathway in the generation of defective retrovirus DNA. J. Virol. **56**:779–789.
47. **Peabody, D. S., and P. Berg.** 1986. Termination-reinitiation occurs in the translation of mammalian cell mRNAs. Mol. Cell. Biol. **6**:2695–2703.
48. **Petersen, R. B., and P. B. Hackett.** 1985. Characterization of ribosome binding on Rous sarcoma virus RNA in vitro. J. Virol. **56**:683–690.
49. **Petersen, R. B., C. H. Hensel, and P. B. Hackett.** 1984. Identification of a ribosome-binding site for a leader peptide encoded by Rous sarcoma virus RNA. J. Virol. **51**:722–729.
50. **Petersen, R. B., A. Moustakas, and P. B. Hackett.** 1989. A mutation in the short 5′-proximal open reading frame on Rous sarcoma virus RNA alters virus production. J. Virol. **63**:4787–4796.
51. **Shank, P. R., and M. Linial.** 1980. Avian oncovirus mutant (SE21Q1b) deficient in genomic RNA: characterization of a deletion in the provirus. J. Virol. **36**:450–456.
52. **Sonstegard, T.** Unpublished data.
53. **Swanstrom, R., H. E. Varmus, and J. M. Bishop.** 1982. Nucleotide sequence of the 5′ noncoding region and part of the *gag* gene of Rous sarcoma virus. J. Virol. **41**:535–541.
54. **Tarpley, W. G., and H. M. Temin.** 1984. The location of v-*src* in a retrovirus vector determines whether the virus is toxic or transforming. Mol. Cell. Biol. **4**:2653–2660.
55. **Wang, E., and A. R. Goldberg.** 1976. Changes in microfilament organization and surface topography upon transformation of chick embryo fibroblasts with Rous sarcoma virus. Proc. Natl. Acad. Sci. USA **73**:4065–4069.
56. **Weller, S. K., A. E. Joy, and H. M. Temin.** 1980. Correlation between cell killing and massive second-round superinfection by members of some subgroups of avian leukosis virus. J. Virol. **33**:494–506.
57. **Wills, J. C., R. C. Craven, and J. A. Achacoso.** 1989. Creation and expression of myristylated forms of Rous sarcoma virus Gag protein in mammalian cells. J. Virol. **63**:4331–4343.
58. **Wu, L.-W.** Unpublished data.